Published in final edited form as:
Neurobiol Dis. 2012 February ; 45(2): 821–828. doi:10.1016/j.nbd.2011.11.006.

Interneuronal calcium channel abnormalities in posttraumatic epileptogenic neocortex

Leonardo C. Faria, **Isabel Parada**, and **David A. Prince**
Department of Neurology and Neurological Sciences, Stanford University School of Medicine, Stanford, California 94305

Abstract

Decreased release probability (Pr) and increased failure rate for monosynaptic inhibitory postsynaptic currents (IPSCs) indicate abnormalities in presynaptic inhibitory terminals on pyramidal (Pyr) neurons of the undercut (UC) model of posttraumatic epileptogenesis. These indices of inhibition are normalized in high [Ca^{++}] ACSF, suggesting dysfunction of Ca^{2+} channels in GABAergic terminals. We tested this hypothesis using selective blockers of P/Q and N-type Ca^{2+} channels whose activation underlies transmitter release in cortical inhibitory terminals. Pharmacologically isolated monosynaptic IPSCs were evoked in layer V Pyr cells by extracellular stimuli in adult rat sensorimotor cortical slices. Local perfusion of 0.2/1 μM ω-agatoxin IVa and/or 1 μM ω-conotoxin GVIA was used to block P/Q and N-type calcium channels, respectively. In control layer V Pyr cells, peak amplitude of eIPSCs was decreased by ~50% after treatment with either 1 μM ω-conotoxin GVIA or 1 μM ω-agatoxin IVa. In contrast, there was a lack of sensitivity to 1 μM ω-conotoxin GVIA in UCs. Immunocytochemical results confirmed decreased perisomatic density of N-channels on Pyr cells in UCs. We suggest that decreased calcium influx via N-type channels in presynaptic GABAergic terminals is a mechanism contributing to decreased inhibitory input onto layer V Pyr cells in this model of cortical posttraumatic epileptogenesis.

Keywords

GABAergic inhibition; injury; N-channels; posttraumatic epilepsy; P/Q-channels

Introduction

Partially isolated neocortical islands (“undercuts or “UCs”) were originally used as an *in vivo* model of chronic epileptogenesis in cats and monkeys (Echlin and McDonald 1954; Grafstein and Sastry 1957; Echlin and Battista 1963) and later successfully adapted for *in vitro* slice experiments in rodents (Prince and Tseng 1993; reviewed in Graber and Prince 2006). Decreased release probability and increased failure rate for monosynaptic and unitary IPSCs in this model of posttraumatic epileptogenesis have suggested abnormal function of presynaptic inhibitory terminals (Faria and Prince 2010; Ma and Prince, 2009). These indices of pyramidal cell (Pyr) inhibition are normalized in high [Ca^{++}] ACSF suggesting

Corresponding address: David Prince, M.D., daprince@stanford.edu, 300 Pasteur Dr. SUMC RM M016, Stanford University, CA 94305-5122, Phone: 650-723-5522, Fax: 650-723-1080.

possible abnormalities in Ca^{++} channels. Presynaptic terminals release neurotransmitters via a calcium-dependent process (Fatt and Katz 1952; Del Castillo and Katz 1954; Catterall and Few 2008), and abnormalities in calcium currents/channels are present in both acute and chronic models of epilepsy (Heinemann and Hamon 1986; Beck et al., 1998) and generalized epilepsies (Fletcher et al., 1996; Burgess et al., 1997; Letts et al., 1998; Barclay et al., 2001).

To date, 5 calcium channel subtypes have been identified: L, R, T, N and P/Q (Tsien et al.,, 1988, 1995; Wheeler et al.,, 1994). The function of P- and Q-types can be investigated selectively as they are blocked by different concentrations of ω-agatoxin IVa (Wheeler et al., 1994), however in most studies the P and Q are considered together as the "P/Q-type" (Wheeler et al., 1996). P/Q and N are the predominant calcium channel subtypes in GABAergic inhibitory terminals of neocortex and hippocampus (Poncer et al., 1997; Rozov et al., 2001; Hefft and Jonas, 2005; Zaitsev et al, 2007; reviewed in Reid et al., 2003). At inhibitory terminals of fast-spiking (FS) interneurons, P/Q-type channels predominate, whereas N-channels are the major subtype expressed in non-FS inhibitory interneurons (Zaitsev et al., 2007; Kruglikov and Rudy 2008). However, P/Q- and N-channels can coexist in a single terminal (Reid et al., 2003, for review) and the identification of interneuronal subtypes solely based on calcium channel expression can be challenging.

We hypothesized that changes in calcium channel subtypes, induced by either lesion or epileptform activity, might alter physiological levels of calcium influx into terminals and contribute to abnormalities in GABAergic transmission in UCs. Direct recordings from presynaptic terminals are restricted to only a few sites in the central nervous system (Zhang and Jackson 1993; Takahashi et al., 1996) and are not feasible in neurons of neocortical slices. We therefore used evoked monosynaptic IPSCs to assess presynaptic function (Murthy et al., 1997; Kravchenko et al., 2006; Faria and Prince 2010). Local perfusion of 0.2–1 μM ω-agatoxin IVa and/or 1 μM ω-conotoxin GVIA was used to block P/Q and N-type calcium channels, respectively. In addition, we used immunocytochemical methods to identify presynaptic GABAergic terminals containing vesicular GABA transporter (VGAT) and co-localized expression of N- and P/Q-channels in controls and UCs. Results suggest that there are decreases in the expression of N-type channels in the chronically injured cortex that would result in decreased GABA release and contribute to hyperexcitability in this model of posttraumatic epileptogenesis.

Methods

Undercut model

All experiments were carried out according to protocols approved by the Stanford Institutional Animal Care and Use Committee. Male Sprague-Dawley rats (P21–22; P0 = date of birth) were deeply anesthetized with ketamine (80 mg/kg ip) and xylazine (Rompun 8 mg/kg ip), and a 3 × 5-mm bone window, centered on the coronal suture and extending medially to within 1 mm of the sagittal suture, was removed, leaving the dura intact and exposing a portion of the sensorimotor cortex unilaterally. Undercuts in the somatosensory cortex of young adult male rats (P21) were made as previously described (Hoffman et al., 1994; Graber and Prince 2006). A 30-gauge needle, bent at approximately a right angle 2.5–3 mm from the tip, was inserted parasagittally 1–2 mm from the interhemispheric sulcus, advanced under direct vision tangentially through the dura and just beneath the pial vessels, and lowered to a depth of 2 mm. The needle then was rotated through 120–135° to produce a contiguous white matter lesion, elevated to a position just under the pia to make a second transcortical cut, and removed. An additional transcortical lesion was placed 2 mm lateral and parallel to the initial parasagittal cut in a similar manner. The skull opening was then covered with sterile plastic wrap (Saran Wrap®), and the skin sutured. Animals were given

carprofen 5 mg/kg sc postoperatively. Lesioned animals recovered uneventfully from surgery and were reanesthetized for slice experiments 2–3 wks later.

Whole cell patch clamp recordings

Male rats were reanesthetized at P35–50 and, using previously described techniques (Faria and Prince 2010), brains were removed and coronal neocortical slices cut and maintained for *in vitro* slice recordings. Neocortical slices (~350 μm) were cut with a vibratome in cold (4 ± 1°C) "slicing" artificial cerebrospinal fluid (ACSF) containing (in mM): 126 NaCl, 2.5 KCl, 1.25 NaH_2PO_4, 1 $CaCl_2$, 2 $MgSO_4$, 26 $NaHCO_3$, and 10 glucose; pH 7.4 when saturated with 95% O_2-5% CO_2. After 1 hr of incubation in standard ACSF containing (in mM) 126 NaCl, 2.5 KCl, 1.25 NaH_2PO_4, 2 $CaCl_2$, 1 $MgSO_4$, 26 $NaHCO_3$ and 10 glucose (33 ± 1°C) single slices were transferred to a recording chamber where they were minimally submerged (33 ± 1°C) and placed on mesh that allowed perfusion of both cut surfaces (Hajos and Mody, 2009) at the rate of 2.5–3 ml/min with standard ACSF containing 5mM KCl to enhance excitability and facilitate population behaviors. Patch electrodes were pulled from borosilicate glass tubing (1.5 mm OD) and had impedances of 2–3 MΩ when filled with intracellular solution containing (in mM): 70 K-gluconate, 70 KCl, 2 NaCl, 10 HEPES, 4 EGTA 4 Mg ATP and 0.3 GTP. The osmolarity of the pipette solution was adjusted to 275–285 mosM with KOH.

Whole cell voltage-clamp recordings were made from visually-identified layer V pyramidal cells using infrared video microscopy and differential interference contrast optics (Zeiss Axioskop2) and a Multiclamp 700A amplifier (Axon Instruments). The estimated chloride equilibrium potential (E_{Cl}) was −16 mV based on the Nernst equation. Access resistance (Ra) was measured in voltage-clamp mode from responses to 2 mV hyperpolarizing voltage pulses using locally available software. Data from recordings in which Ra varied by more than 15% or was > 15 MΩ were rejected. Pyr neurons were identified as cells with large somata and a single emerging apical dendrite extending toward the pial surface. In addition, in some slices, intracellular labeling with biocytin was used to confirm cell type and position. Pharmacologically isolated (monosynaptic) IPSCs were reliably evoked with monopolar tungsten stimulating electrodes, placed in layer V, ~ 100 μm below the recorded Pyr soma to obtain steep input/output slopes (Salin and Prince, 1996). 2-amino-5-phosphonovaleric acid (D-AP5; 50 μM) and 6,7-Dinitroquinoxaline-2,3-dione (DNQX; 20 μM) (Ascent Scientific) in ACSF were continuously applied via bath perfusion. The time for drug wash in was typically < 5min, as judged by alterations in peak amplitude of the evoked (e)EPSCs. ω-conotoxin GVIA (1 μM; Ascent Scientific) and ω-agatoxin IVa (0.2–1 μM; Bachem Bioscience) were applied over 10 min (~0.5ml/min) through a small teflon tube placed adjacent to the soma of the recorded layer V Pyr cell. Although locally applied, solutions containing toxins were observed to spread across all cortical layers.

To obtain the threshold (T) for evoking IPSCs, the stimulus duration was initially set at 100 μs and stimulus current increased until a stable IPSC with a failure rate ≤50% was evoked. The pulse duration was then increased to 150 μs (1.5T) for determination of peak amplitude. In some experiments, bath perfusion of gabazine (10 μM) was used to block the evoked events and verify that they were mediated by $GABA_A$ receptors (not shown). Responses in which spontaneous (s) IPSCs were superimposed on evoked IPSCs were not included in the data.

Baseline values for eIPSC peak amplitude were obtained in control and UC rats during the first 5min of stable whole cell recording in standard ACSF. This was followed by a single 10min local perfusion of ω-agatoxin IVa and/or ω-conotoxin GVIA. The effects of calcium channel blockade on eIPSCs were routinely assessed over 5 min, beginning after the end of toxin perfusion. To determine whether effects of toxin were reversible, or changing over

time, in some experiments Pyr cells were continuously recorded for ~ 1h following brief 10 min toxin perfusion, followed by ACSF wash. In agreement with previous results (Tsien et al., 1988; Williams et al., 1992; Ali and Nelson, 2006), the effects of toxin on eIPSC peak amplitude were stable and not reversible during prolonged recordings. Thus, a single 10 min local perfusion was considered to be equivalent to continuous toxin exposure. Mean values for peak amplitude were calculated by averaging eIPSCs over 5min prior to, and after the 10 min toxin treatment in control and UC (unless otherwise noted). Statistical significance was determined with two-tailed Student's *t*-test ($P < 0.05$). Data are expressed as means ± SE and "n" corresponds to the number of neurons (unless otherwise noted). One neuron was recorded per slice and no more than 2 slices were used per rat. "Baseline" values below are those for either control naïve rats or for UCs before toxin exposure.

Immunocytochemistry

P35–50 male rats were deeply anesthetized with Beuthanasia-D (110mg/Kg) and perfused transcardially with 4 % paraformaldehyde. Coronal brain sections (40 μm) were cut with a microtome (Microm, HM 400; Heidelberg). Free floating sections were incubated for 1h in 10% normal goat serum in phosphate buffered saline (PBS), followed by 48h incubation with the primary antibodies against N-channel (1:200) or P/Q-channel (1:200) (Alomone Labs, Israel and Sy Sy Germany, respectively) in combination with an antibody for vesicular GABA transporter (VGAT) (Sy Sy Germany; 1:500) diluted in PBS containing 0.3% (v/v) Triton X-100. Additional sections were similarly processed and incubated with primary antibodies against cholecystokinin (CCK, 1:500, CURE). Subsequently, slices were rinsed in PBS and incubated for 2h with the corresponding fluorescent secondary antibodies (Jackson Immuno Research Laboratories). Sections were mounted on slides using Vectashield Mounting Media (Burlingame, CA). Images were captured with a laser scanning confocal microscope (Zeiss LSM 510) by using a 63x oil immersion lens and a zoom factor of 2. Secondary antibodies tagged to Fluorescein 488 and Cy3 were excited with 488- and 543- nm lasers and observed, through 510–530 and 560–615 emission filters, respectively. A pinhole of 1 airy unit and identical settings for detector gain and amplifier offset were used to capture all confocal images.

Quantification of immunoreactivity (IR) for the antibodies against N- or P/Q-channels + VGAT, and CCK was performed in terminals projecting onto the soma of layer V Pyr cells. For volumetric analysis of objects near the Pyr cell somata, Pyr cells were first identified in confocal image stacks as triangular shaped neurons with an apical dendrite projecting towards the pial surface. Cells whose apical dendrite could not be identified were not included in the analyses. The image stack containing CCK-IR was scanned and cropped in the z-direction to encompass several sequential images through the center of the Pyr cell somata, and a region of interest (ROI) was manually drawn around the perisomatic region. The inner boundary was drawn at the junction of positive perisomatic immunostaining and the void representing the cell body. The outer boundary was drawn to include immunoreactive puncta in close apposition to the soma (this resulted in roughly a 3 – 5 μm wide "train track" around the perisomatic region that extended several μm in the z-direction. Objects within the ROI for a given channel (e.g.. cy-3 tagged perisomatic proteins) were identified by using Volocity software (Improvision) if their pixel intensities were greater than 2 standard deviations away from the mean pixel intensity and the voxel size was >0.2 μm^3. The cumulative volume of the identified objects (i.e. the cumulative volume of the perisomatic protein of interest within the ROI) was compared to the total volume of the ROI. Thus, the perisomatic protein expression was represented as a fraction of ROI volume.

Co-localization of IR for P/Q- or N-type channels with the presynaptic marker VGAT was also analyzed in the perisomatic ROI of layer V Pyr cells. However, due to the limited penetration of antibodies against P/Q- and N-channels, quantification of calcium channel-IR

was performed in single confocal sections using Image J (NIH). Results show the percentage of colocalized pixels per area of ROI in layer V Pyr cells. Adjustments of contrast and size were equally applied to some images from control and UC cortices as noted in figure legends.

Results

Whole cell recordings acceptable for analysis were obtained from layer V Pyr cells in slices from 16 control rats (n = 20 cells) and from slices cut through the partial cortical isolations in 19 rats (23 cells). The properties of pharmacologically isolated monosynaptic eIPSCs (Methods) were examined at a holding potential (V_h) of −60mV. In some slices, spontaneous and evoked events were initially recorded from layer V Pyr neurons in standard ACSF without glutamatergic blockade. Under these conditions (E_{Cl} -16 mV, V_h, −60 mV), spontaneous and evoked epileptform “burst like” events, likely consisting of mixed EPSCs and IPSCs, were recorded in neurons of undercut slices (not shown; Faria and Prince 2010).

Presynaptic P/Q and N-type channels mediate GABA release onto control layer V Pyr cells

To identify the calcium channel subtypes present in inhibitory presynaptic terminals, we tested the sensitivity of monosynaptic eIPSCs recorded in control layer V Pyr cells to a co-application of 1 μM ω-conotoxin GVIA and 0.2/1 μM ω-agatoxin IVa (N- and P/Q-calcium channel blockers, respectively). Baseline mean peak amplitude of control eIPSCs (184.3 ± 40.2pA) decreased to 13.8 ± 5.9pA (Fig. 1; $P < 0.005$; n = 8) after combined N- and P/Q-channel blockade. Block was complete in 6 neurons and incomplete in 2 cells where eIPSC peak amplitude was reduced to 29 and 23% of baseline. These results suggest that P/Q- and N-type are the predominant Ca^{++} channels in inhibitory terminals of most presynaptic GABAergic interneurons. The failure to completely block eIPSCs in 2 cells (Fig. 1A) could have resulted either from incomplete penetration and delayed effects of toxins or the presence of another subtype of Ca^{++} channel in some interneurons (Kamp et al., 2005). As previously reported (see references in Methods), the effects of a co-application of 1 μM ω-conotoxin GVIA and 0.2/1 μM ω-agatoxin IV on eIPSCs were irreversible during subsequent wash with ACSF (Fig. 1B) for as long as the Pyr neuron was recorded (> 1 h in some cells). In addition, we found no shifts in holding current when the toxins were applied, suggesting that significant postsynaptic conductances were not affected.

Differences in ω-conotoxin effects on eIPSCs in Pyr cells from controls and UCs

The contribution of N-type channels to presynaptic GABA release in control rats was analyzed by comparing whole cell recordings of IPSCs evoked by 1.5T stimuli in 10 layer V Pyr cells before and after treatment with 1 μM ω-conotoxin GVIA. Average baseline peak amplitude of control eIPSCs (164.3 ± 34.4pA) decreased after N-channel blockade to 74.3 ± 16.2pA ($P < 0.005$; Fig. 2A, left), suggesting that the remaining fraction of eIPSC current was mediated by a different calcium channel subtype, presumably P/Q channels (Fig. 1). In contrast, mean peak amplitude obtained in neurons of UCs following 1 μM ω-conotoxin GVIA (123.9 ± 16.2; n = 13) was not significantly different from baseline values (136 ± 13.7pA, paired t-test: $P > 0.05$; Fig 2A, right). To assess differences in sensitivity to 1 μM ω-conotoxin GVIA, we normalized peak amplitude of eIPSCs (shown in Fig 2A) and compared the % changes following treatment in control vs. UCs. In control, mean peak amplitude decreased to 54.8 ± 6.4% of baseline values following toxin perfusion. In contrast, baseline mean peak amplitude of eIPSC in UCs decreased only 8.38 ± 8.6% after treatment (unpaired t-test; $P < 0.0005$; Fig. 2B). Results suggested decreased expression of N-type channels in axons of interneurons of epileptogenic neocortex, or alterations that rendered these channels unresponsive to ω-conotoxin GVIA.

To rule out decreased toxin penetration into the slices from chronically injured cortex, the effects of N-channel blockade on eIPSCs after ω-conotoxin GVIA exposure were evaluated during prolonged continuous recordings in 3 layer V Pyr cells, from 3 different UCs. Baseline mean peak amplitude of eIPSCs (189.2 ± 27.8 pA) was unaltered when assessed 30min after the onset of 1 μM conotoxin GVIA perfusion (195 ± 19.6 pA; $P > 0.05$). In contrast, mean peak amplitude of eIPSC in 3 control neurons decreased from a baseline of 140 ± 24.2 pA to 60.4 ± 6.9 pA after N-channel blockade over the same time interval ($P < 0.05$). Results suggest that the apparent lack of effect of N-channel blockade on eIPSCs in UC Pyr cells was due to changes in contribution of presynaptic N-channels to the evoked IPSCs, rather than to slow penetration of the slice by the toxin. Loss of potency of the toxin in these experiments was not a factor as the same batch of toxin on the same day blocked N channels in control cells.

ω-agatoxin IVa effects on eIPSC amplitude in Pyr cells from controls and UCs

Evoked monosynaptic IPSCs were recorded in 7 control layer V Pyr cells under the conditions described above. To assess the effects of P/Q-channel blockade on eIPSCs, baseline mean peak amplitude was recorded and compared to values obtained following 0.2 μM ω-agatoxin IVa. Mean peak amplitude of eIPSCs decreased significantly from a baseline of 127.2 ± 18.6 pA to 59.7 ± 9.6 pA following P/Q-channel blockade ($P < 0.01$; Fig 3A, left). To test the effects of a higher (1 μM) concentration of ω-agatoxin IVa on eIPSC peak amplitude, 3 additional control layer V Pyr cells were recorded at baseline and 30 min after toxin treatment. Under these conditions, mean peak amplitude of baseline control eIPSC (149.8 ± 12.2pA) decreased to 80 ± 7.6pA after treatment ($P < 0.005$), or to about the same extent as occurred with the lower toxin concentration.

We compared the above effects of ω-agatoxin IVa in controls to those in Pyr cells in slices from UC rats. Local perfusion of 0.2μM ω-agatoxin IVa decreased mean peak eIPSC amplitude in UCs from 112.7 ± 20.8 pA at baseline to 41.2 ± 5.9 pA measured following toxin exposure ($n = 5$; $P < 0.05$; Fig 3A, right).

GABA release from N and P/Q channel activation in controls normally accounted for almost all of the eIPSC current (Fig. 1) and N channel function was markedly decreased in the UC (Fig. 2). Therefore, in the absence of a compensatory increase in other presynaptic Ca^{++} channels (e.g. Grimm et al., 2008), blockade of the remaining P/Q channels with ω-agatoxin IVa would be expected to markedly decrease or eliminate eIPSCs.

Prolonged recordings of eIPSCs from Pyr neurons in UC slices, over ~25min after exposure to 1 μM ω-agatoxin IVa, showed that full effects of toxin treatment were slow to develop (Fig. 3B, filled circles). Under these conditions, eIPSCs were completely blocked in 5 out of 6 Pyr cells (i.e. not > 3x RMS of baseline noise). Incomplete blockade in a single cell contributed to the small fraction of mean eIPSC amplitude after 20 min of toxin exposure shown in Fig 3B, perhaps due to the presence of residual N- or other Ca^{++} channels in terminals. Increasing the stimulus strength to 2.5–3T did not evoke detectable eIPSCs once full blockade of eIPSCs occurred ($n = 3$ cells from 2 UC rats; Fig 3B, inset). The loss of eIPSCs in injured Pyr cells was not due to alterations in the quality of recordings, as access resistance did not change significantly during these prolonged recordings. These data suggest that there is a relative sparing of P/Q-channel dependent inhibitory transmission in UC slices, while N-channel dependent transmission is primarily affected. To further evaluate these electrophysiological results, we used immunocytochemical techniques to assess P/Q- and N-channel proteins in interneuronal terminals.

P/Q- and N-type channel protein immunoreactivity in control and UCs

We used layer V Pyr neuron perisomatic VGAT immunoreactivity (IR) to image presynaptic GABAergic terminals (Chaudhry et al., 1998) and dual IR for VGAT and N- or P/Q channels to identify calcium channels present in inhibitory terminals (Grimm et al., 2008). Confocal images of sections reacted for VGAT and N-current channel IR were obtained in controls (n = 13 cells, 3 rats) and UCs (n = 8 cells, 3 rats). Images from control (Fig. 4A, A1) show colocalization (yellow) of N-type channel-IR (green) and VGAT-IR (red) in the perisomatic area of layer V Pyr cells. In contrast, there was decreased expression of N-type channels and little colocalization of VGAT/N-channel-IR in inhibitory presynaptic terminals in UCs (Fig. 4B, B1). To measure differences between control and UC, we compared the area of co-localized VGAT- and N-channel-IR in the perisomatic ROI of layer V Pyr cells (Methods). To compensate for differences in cell size (Prince and Tseng, 1993), results from control and UCs were normalized and compared as shown in Fig. 4C. Total area of the ROI was 4978 ± 42.5 μm^2 in control (n = 13) and 1494.6 ± 118.8 μm^2 in UC (n = 8). Immunoreactivity for N-channel co-localized with VGAT in the ROI in control (20 ± 2.2%) was significantly greater than UCs (5.4 ± 1.8%, unpaired t-test; P > 0.0001).

To determine whether there was a compensatory increase in P/Q channel expression in UCs (Grimm et al., 2008), channel density in inhibitory presynaptic terminals of control and UCs was assessed as above by measuring the colocalization of IR for VGAT and P/Q-channels.

As shown in Fig. 5, both VGAT- and P/Q-IR were prominent perisomatically around layer V Pyr cells. Co-localized P/Q- and VGAT-IR in control (n = 8, ROI area = 1905.36 ± 223.8 μm^2; Fig. 5A) and UC cells (n = 12, ROI area = 1101.8 ± 92.9 μm^2; Fig. 5B), corresponded respectively to 14.5 ± 1.8% and 14.9 ± 2.2% of the total perisomatic ROI (Fig. 5C; unpaired t-test: P > 0.05) (Methods). These results suggest that there was no significant change in the expression of P/Q-channels in inhibitory presynaptic terminals of somatically-targeting interneurons in the UC.

The interneuronal source of the perisomatic GABAergic terminals that showed a decrease in N- but not P/Q-current channel-IR in these experiments might be either parvalbumin (PV)- or cholecystokinin (CCK)-containing-containing basket cells that target pyramidal cells in neocortex (Figs. 4A, 5A) and hippocampus (Pawelzic et al, 2002; Karson et al, 2009; Lee and Soltesz, 2011). CCK interneurons are low in density in layer V, while PV basket cells are abundant (2.9% and 52.7% of Venus-labeled interneurons, respectively in Uematsu et al, 2008). In hippocampus (Poncer et al, 1997; Hefft and Jonas, 2005) and layer II-III of neocortex (Zaitsev et al, 2007), P/Q- and N-current channels are segregated in terminals of parvalbumin and CCK-containing interneurons, respectively, suggesting that loss or injury of CCK neurons or terminals in the UC, as occurs in hippocampus in the pilocarpine model of epileptogenesis (Wyeth et al, 2010), could result in the decreased N current channel-IR. However, different channel subtypes may coexist in the terminals of the same neuron (Doze et al, 1995; Mintz et al, 1995; Wheeler et al, 1996; Wilson et al, 2001), which raises the possibility that axons of PV-containing basket cells in neocortical layer V could possess both P/Q and N- channels and alterations in them might contribute to the loss of sensitivity to ω-conotoxin GVIA and reduction in N-channel-IR.

We assessed the volume of inhibitory terminals containing CCK-IR in the perisomatic area of layer V Pyr cells using z-stacks of confocal images and Volocity software (Methods). In control, mean perisomatic volume of the ROI containing puncta around layer V Pyr cells (n = 12 cells, 3 rats) was 2020.9 ± 404.9 μm^3. Mean volumes of IR corresponding to CCK around these cells was 47 ± 12 μm^3. In agreement with an earlier observation on the decreased size of Pyr cell somata in the UC (Prince and Tseng, 1993), mean perisomatic volume of Pyr cells decreased to 1101.8 ± 92.9 μm^3 (n = 12 cells, 3 rats, unpaired t-test; P <

0.05). Mean volume of perisomatic IR for CCK in UC cells was 31.1 ± 8.6 μm^3. To compensate for differences in cell volume, quantification of CCK-IR in UC was normalized and compared to control. The percentage of CCK-IR observed in control Pyr cells (2.1 ± 0.4%, n = 12) was similar to that present in UC cells (2.9 ± 0.4%, n = 11; P > 0.05). These results, suggest that CCK-IR is present in inhibitory terminals projecting onto the perisomatic area of Pyr cells of the UC.

Discussion

We used whole cell recordings and analysis of immunoreactivity to investigate the function and expression of P/Q- and N-type channels in presynaptic terminals of control and UC GABAergic interneurons projecting onto layer V Pyr cells. Results showed that P/Q- and N-type channels are expressed in inhibitory presynaptic terminals and contribute similarly to eIPSCs recorded in control layer V Pyr cells. In contrast, inhibitory presynaptic terminals in UC cortex have significant decreases in density and function of N-type calcium channels (Figs. 2, 4). There were no indications of a compensatory increase in the density of P/Q-channels in terminals in the epileptogenic cortex. Although postsynaptic calcium channels can influence elimination of synapses during development (Hashimoto et al., 2011), the lack of shifts in holding currents in layer V pyr cells after toxin exposure and results of numerous experiments (e.g. Evans and Zamponi, 2006; Kuglikov and Rudy, 2008; Poncer et al, 1997;) suggests that toxin-sensitive P/Q- and N-channels are located in presynaptic terminals.

P/Q- and N-channels are present in control inhibitory presynaptic terminals

The factors that determine the expression of a calcium channel subtype in a presynaptic terminal are not fully understood, but they might be influenced by the identity of the postsynaptic cell. This proposal is supported by observations that different release probabilities (Scanziani et al., 1998) and different types of calcium channels (Reuter 1995; Rozov et al., 2001; Reid et al., 2003) can be present in different terminals of the same cell. Thus, retrograde signaling from the target neuron might influence the expression of a specific calcium channel subtype in a presynaptic terminal. In this connection, it is important to note that there are both structural and functional alterations in the axotomized layer V Pyr cells in the UC cortex (Prince and Tseng 1993; Salin et al., 1995; Tseng and Prince 1996; Prince et al., 2009) that could influence expression of retrograde signals onto inhibitory interneurons (e.g., Kohara et al., 2007) and alter expression of presynaptic Ca^{++} channels (e.g.Baldelli et al, 2005).

Our results in control layer V Pyr neurons indicate that activation of N- and P/Q-type channels can contribute similarly to the eIPSC, however the use of monosynaptic rather than uIPSCs as an index response precludes further analysis of the inhibitory cell types involved, or the distribution of P/Q and N-type channels on single presynaptic interneurons (see Reid et al., 2003 for review). In FS cells, P/Q-type is predominant whereas N-channel is the major subtype expressed in non-FS terminals (Zaitsev et al., 2007; Kruglikov and Rudy 2008). The similar contribution from P/Q- and N-channels to monosynaptic IPSCs in control is in agreement with the observation that FS cells correspond to approximately 50% of all interneurons in the cerebral cortex (reviewed in Markram et al., 2004; Uematsu et al., 2008). However, classification of interneuronal subtypes by selective calcium channel expression might be challenging since these channels can coexist in the same terminal (Reid et al., 2003). The results reported in this study suggest that presynaptic calcium influx is mediated by P/Q- and N-channels in control, however, as indicated above, it is not clear to what extent these channels are present in terminals from different cell types or may coexist in the same or different terminals of the same presynaptic cell. Although extracellular stimulation close to cell soma favors the activation of FS interneurons, it is likely that more distally targeted elements are also contributing to eIPSCs recorded in layer V Pyr cells. The slower rise time

for responses to 1.5 T vs T stimuli in UCs (Faria and Prince 2010) is compatible with this conclusion. The use of paired recordings will be helpful to further investigate this issue.

To confirm results obtained with whole cell recordings, we performed immunocytochemical analyses with antibodies against P/Q- and N-channels and the vesicular GABA transporter VGAT in control and undercut sections. As expected, there was perisomatic expression of boutons containing VGAT in controls, presumably arising predominantly from FS interneurons (Somogyi et al., 1998; Prince et al., 2009), co-localized with P/Q- (Fig. 5A) and N-type channels (Fig. 4A). Therefore, electrophysiological and anatomical data are in agreement and suggest that P/Q- and N-channels mediate calcium influx into perisomatic inhibitory terminals that are derived predominantly from FS cells in control rats.

Loss of N-type channels in injured presynaptic terminals

The lack of effects of ω-conotoxin GVIA on eIPSCs recorded in injured Pyr cells together with the immunocytochemical results, indicate that there are structural and functional abnormalities in N-type Ca^{++} channels in GABAergic interneurons in this model of posttraumatic epileptogenesis. These changes likely translate to decreased inhibition due to the lack of depolarizing GABAergic effects in this model (Hoffman et al. 1994; Jin et al, 2005). However, we cannot rule out sufficient shifts in E_{Cl} to render GABAergic transmission depolarizing during intense prolonged epileptiform discharges, or at a short latency after injury. Decreased density of N-type channel ($Ca_V2.2$) has been reported in the hilus of dentate gyrus and in the stratum pyramidale of CA3 area following pilocarpine-induced status epilepticus (Xu et al., 2010). Moreover, CCK-containing basket cells expressing N-type calcium channels, but not PV-containing cells, were selectively reduced in a model of temporal lobe epilepsy (Wyeth et al., 2010). Decreased density of N-channels and reduced sensitivity to N-channel blockade has also been observed after axotomy of small dorsal root ganglion neurons (Fuchs et al., 2007). The consequences of decreased expression of N-type channels on circuit excitability are complex, difficult to predict and depend on compensatory mechanisms in other calcium channel subtypes. For example, calcium channel loss in excitatory versus inhibitory terminals is likely to induce contrasting effects on circuit excitability. Also, blockade of N-channels can prevent injury-induced glutamate release in a model of traumatic brain injury (Shahlaie et al., 2010). In contrast, N-channel loss in injured presynaptic inhibitory terminals might contribute to decreased release probability of GABA and increased failure rate for eIPSCs in UCs (Faria and Prince 2010; Ma and Prince 2009).

As a consequence of N-channel loss, eIPSCs recorded in injured layer V Pyr cells were predominantly mediated by P/Q-channels (Fig. 3B). Thus, it is likely that injury and/or alterations in cortical activity affected N-channels preferentially, while P/Q-channels were preserved.

Lack of compensatory mechanisms in P/Q-channels in UCs

The absence of a calcium channel subtype in a terminal is often compensated for by the increased density of other subtypes to maintain physiological levels of neurotransmission at synapses. This phenomenon occurs in terminals from different cell types in diverse areas and is evident in P/Q- and N-channels of cultured hippocampal neurons (Grimm et al., 2008), mice lacking N-channels (Takahashi et al., 2004) and in excitatory cerebrocortical terminals (Ladera et al., 2009). Our data do not support such a compensatory up-regulation of P/Q expression in perisomatic terminals in this model of cortical injury (Fig. 5). Compensatory mechanisms, if present, would not necessarily restore physiological synaptic transmission, as P/Q- and N-type channels have contrasting functional properties that might translate to different roles in transmitter release (Zhang et al., 1996; Wu et al., 1999; Martín

et al., 2007; Zaitsev et al., 2007). In contrast to the decreased inhibitory connectivity (Faria and Prince, 2010; Jin et al 2011) and N-channel density (Fig. 4B,C), The density of CCK-containing terminals projecting to somata of layer V Pyr cells appears to be unchanged in UCs. CCK-IR in dendritically targeting terminals (e.g. Pawelzik et al, 2002) was not included in our analysis. Our results indicate that abnormalities in UCs might be restricted to terminals containing N-type calcium channels, However, it is important to note that other types of calcium channels may be affected in other models of epileptogenesis (Becker et al., 2008) or human epileptic brain (Jouvenceau et al., 2001).

Acknowledgments

Funding: This work was supported by National Institute of Health (NS39579 and NS12151 from the NINDS). We thank Dr. Daniel Koji Takahashi for his helpful comments.

References

Ali AB, Nelson C. Distinct Ca2+ channels mediate transmitter release at excitatory synapses displaying different dynamic properties in rat neocortex. Cereb Cortex. 2006; 16(3):386–9. [PubMed: 15917483]

Barclay J, Balaguero N, Mione M, Ackerman SL, Letts VA, Brodbeck J, Canti C, Meir A, Page KM, Kusumi K, Perez-Reyes E, Lander ES, Frankel WN, Gardiner RM, Dolphin AC, Rees M. Ducky mouse phenotype of epilepsy and ataxia is associated with mutations in the Cacna2d2 gene and decreased calcium channel current in cerebellar Purkinje cells. J Neurosci. 2001; 21:6095–6104. [PubMed: 11487633]

Baldelli P, Novara M, Carabelli V, Hernandez-Guijo JM, Carbone E. BDNF up-regulates evoked GABAergic transmission in developing hippocampus by potentiating presynaptic N- and P/Q-type Ca2+ channels signalling. Eur J Neurosci. 2002; 16:2297–2310. [PubMed: 12492424]

Beck H, Steffens R, Elger CE, Heinemann U. Voltage-dependent Ca2+ currents in epilepsy. Epilepsy Res. 1998; 32:321–332. [PubMed: 9761331]

Becker AJ, Pitsch J, Sochivko D, Opitz T, Staniek M, Chen CC, Campbell KP, Schoch S, Yaari Y, Beck H. J Neurosci. 2008; 28:13341–53. [PubMed: 19052226]

Burgess DL, Jones JM, Meisler MH, Noebels JL. Mutation of the Ca2+ channel b subunit gene Cchb4 is associated with ataxia and seizures in the lethargic (lh) mouse. Cell. 1997; 88:385–392. [PubMed: 9039265]

Catterall WA, Few AP. Calcium channel regulation and presynaptic plasticity. Neuron. 2008; 59:882–901. [PubMed: 18817729]

del Castillo J, Katz B. Quantal components of the end-plate potential. J Physiol. 1954; 124:560–73. [PubMed: 13175199]

Chaudhry FA, Reimer RJ, Bellocchio EE, Danbolt NC, Osen KK, Edwards RH, Storm-Mathisen J. The vesicular GABA transporter, VGAT, localizes to synaptic vesicles in sets of glycinergic as well as GABAergic neurons. J Neurosci. 1998; 18(23):9733–50. [PubMed: 9822734]

Doze VA, Cohen GA, Madison DV. Calcium channel involvement in GABAB receptor-mediated inhibition of GABA release in area CA1 of the rat hippocampus. J Neurophysiol. 1995; 74:43–53. [PubMed: 7472344]

Echlin FA, Battista A. Epileptform seizures from chronic isolated cortex. Arch Neurol. 1963; 9:154–70. [PubMed: 14048164]

Echlin FA, McDonald J. The supersensitivity of chronically isolated and partially isolated cerebral cortex as a mechanism in focal cortical epilepsy. Trans Am Neurol Assoc. 1954; 13:75–9. [PubMed: 13238319]

Evans RM, Zamponi GW. Presynaptic Ca2+ channels--integration centers for neuronal signaling pathways. Trends Neurosci. 2006; 29:617–24. [PubMed: 16942804]

Faria LC, Prince DA. Presynaptic inhibitory terminals are functionally abnormal in a rat model of posttraumatic epilepsy. J Neurophysiol. 2010; 104:280–290. [PubMed: 20484536]

Fatt P, Katz B. Spontaneous subthreshold activity at motor nerve endings. J Physiol. 1952; 117:109–128. [PubMed: 14946732]

Fletcher CF, Lutz CM, O'Sullivan TN, Shaughnessy JD Jr, Hawkes R, Frankel WN, Copeland NG, Jenkins NA. Absence epilepsy in tottering mutant mice is associated with calcium channel defects. Cell. 1996; 87:607–17. [PubMed: 8929530]

Fuchs A, Rigaud M, Sarantopoulos CD, Filip P, Hogan QH. Contribution of calcium channel subtypes to the intracellular calcium signal in sensory neurons: the effect of injury. Anesthesiology. 2007; 107:117–27. [PubMed: 17585223]

Graber, KD.; Prince, DA. Chronic partial cortical isolation. In: Pitkanen, A.; Schwartzkroin, P.; Moshe, S., editors. Models of Seizures and Epilepsy. Elsevier; San Diego: 2006. p. 477-493.

Grafstein B, Sastry PB. Some preliminary electrophysiological studies on chronic neuronally isolated cerebral cortex. Electroencephalogr Clin Neurophysiol. 1957; 4:723–5. [PubMed: 13480247]

Grimm C, Holter NI, Draguhn A, Bruehl C. Compensatory increase in P/Q-calcium current-mediated synaptic transmission following chronic block of N-type channels. Neurosci Lett. 2008; 442:44–9. [PubMed: 18602451]

Hájos N, Mody I. Establishing a physiological environment for visualized in vitro brain slice recordings by increasing oxygen supply and modifying aCSF content. J Neurosci Methods. 2009; 183:107–13. [PubMed: 19524611]

Hashimoto K, Tsujita M, Miyazaki T, Kitamura K, Yamazaki M, Shin HS, Watanabe M, Sakimura K, Kano M. Postsynaptic P/Q-type Ca2+ channel in Purkinje cell mediates synaptic competition and elimination in developing cerebellum. Proc Natl Acad Sci USA. 2011; 108(24):9987–92. [PubMed: 21628556]

Hefft S, Jonas P. Asynchronous GABA release generates long-lasting inhibition at a hippocampal interneuron-principal neuron synapse. Nat Neurosci. 2005; 8:1319–28. [PubMed: 16158066]

Heinemann U, Hamon B. Calcium and epileptogenesis. Exp Brain Res. 1986; 1:1–10. [PubMed: 3026832]

Hoffman SN, Salin PA, Prince DA. Chronic neocortical epileptogenesis in vitro. J Neurophysiol. 1994; 71:1762–1773. [PubMed: 8064347]

Jin X, Huguenard JR, Prince DA. Impaired Cl- extrusion in layer V pyramidal neurons of chronically injured epileptogenic neocortex. J Neurophysiol. 2005; 93:2117–26. [PubMed: 15774713]

Jin X, Huguenard JR, Prince DA. Reorganization of inhibitory synaptic circuits in rodent chronically injured epileptogenic neocortex. Cereb Cortex. 2011; 21:1094–104. [PubMed: 20855494]

Jouvenceau A, Eunson LH, Spauschus A, Ramesh V, Zuberi SM, Kullmann DM, Hanna MG. Human epilepsy associated with dysfunction of the brain P/Q-type calcium channel. Lancet. 2001; 358:801–807. [PubMed: 11564488]

Kamp MA, Krieger A, Henry M, Hescheler J, Weiergräber M, Schneider T. Presynaptic 'Ca2.3-containing' E-type Ca channels share dual roles during neurotransmitter release. Eur J Neurosci. 2005; 21:1617–25. [PubMed: 15845089]

Karson MA, Tang AH, Milner TA, Alger BE. Synaptic cross talk between perisomatic-targeting interneuron classes expressing cholecystokinin and parvalbumin in hippocampus. J Neurosci. 2009; 29:4140–54. [PubMed: 19339609]

Kohara K, Yasuda H, Huang Y, Adachi N, Sohya K, Tsumoto T. A local reduction in cortical GABAergic synapses after a loss of endogenous brain-derived neurotrophic factor, as revealed by single-cell gene knock-out method. J Neurosci. 2007; 27:7234–7244. [PubMed: 17611276]

Kravchenko MO, Moskalyuk AO, Fedulova SA, Veselovsky NS. Calcium-dependent changes of paired-pulse modulation at single GABAergic synapses. Neurosci Lett. 2006; 395:133–7. [PubMed: 16321469]

Kruglikov I, Rudy B. Perisomatic GABA release and thalamocortical integration onto neocortical excitatory cells are regulated by neuromodulators. Neuron. 2008; 58:911–24. [PubMed: 18579081]

Ladera C, Martín R, Bartolomé-Martín D, Torres M, Sánchez-Prieto J. Partial compensation for N-type Ca(2+) channel loss by P/Q-type Ca(2+) channels underlines the differential release properties supported by these channels at cerebrocortical nerve terminals. Eur J Neurosci. 2009; 29:1131–40. [PubMed: 19302149]

Lee SY, Soltesz I. Cholecystokinin: a multi-functional molecular switch of neuronal circuits. Dev Neurobiol. 2011; 71:83–91. [PubMed: 21154912]

Letts VA, Felix R, Biddlecome GH, Arikkath J, Mahaffey CL, Valenzuela A, Bartlett FS 2nd, Mori Y, Campbell KP, Frankel WN. The mouse stargazer gene encodes a neuronal Ca2+-channel gamma subunit. Nat Genet. 1998; 19:340–7. [PubMed: 9697694]

Ma Y, Prince DA. Decreased inhibition in chronically epileptogenic neocortex due to abnormalities in presynaptic terminals of fast-spiking interneurons (Abstract). Epilepsia. 2009; 50:23.

Markram H, Toledo-Rodriguez M, Wang Y, Gupta A, Silberberg G, Wu C. Interneurons of the neocortical inhibitory system. Nat Rev Neurosci. 2004; 5:793–807. [PubMed: 15378039]

Martín R, Torres M, Sánchez-Prieto J. mGluR7 inhibits glutamate release through a PKC-independent decrease in the activity of P/Q-type Ca2+ channels and by diminishing cAMP in hippocampal nerve terminals. Eur J Neurosci. 2007; 26:312–22. [PubMed: 17650109]

Mintz IM, Sabatini BL, Regehr WG. Calcium control of transmitter release at a cerebellar synapse. Neuron. 1995; 15:675–688. [PubMed: 7546746]

Murthy VN, Sejnowski TJ, Stevens CF. Heterogeneous release properties of visualized individual hippocampal synapses. Neuron. 1997; 18:599–612. [PubMed: 9136769]

Pawelzik H, Hughes DI, Thomson AM. Physiological and morphological diversity of immunocytochemically defined parvalbumin- and cholecystokinin-positive interneurones in CA1 of the adult rat hippocampus. J Comp Neurol. 2002; 443:346–67. [PubMed: 11807843]

Poncer JC, McKinney RA, Gähwiler BH, Thompson SM. Either N- or P-type calcium channels mediate GABA release at distinct hippocampal inhibitory synapses. Neuron. 1997; 18:463–72. [PubMed: 9115739]

Prince DA, Parada I, Scalise K, Graber K, Jin X, Shen F. Epilepsy following cortical injury: cellular and molecular mechanisms as targets for potential prophylaxis. Epilepsia. 2009; 50:30–40. [PubMed: 19187292]

Prince DA, Tseng GF. Epileptogenesis in chronically injured cortex: in vitro studies. J Neurophysiol. 1993; 69:1276–1291. [PubMed: 8492163]

Reid CA, Bekkers JM, Clements JD. Presynaptic Ca2+ channels: a functional patchwork. Trends Neurosci. 2003; 26:683–7. [PubMed: 14624853]

Reuter H. Measurements of exocytosis from single presynaptic nerve terminals reveal heterogeneous inhibition by Ca(2+)-channel blockers. Neuron. 1995; 14:773–9. [PubMed: 7718239]

Rozov A, Burnashev N, Sakmann B, Neher E. Transmitter release modulation by intracellular Ca2+ buffers in facilitating and depressing nerve terminals of pyramidal cells in layer 2/3 of the rat neocortex indicates a target cell-specific difference in presynaptic calcium dynamics. J Physiol. 2001; 531:807–26. [PubMed: 11251060]

Salin PA, Prince DA. Electrophysiological mapping of GABAA receptor-mediated inhibition in adult rat somatosensory cortex. Neurophysiol. 2006; 75(4):1589–600.

Salin PA, Tseng GF, Hoffman SN, Parada I, Prince DA. Axonal sprouting in layer V pyramidal neurons of chronically injured cerebral cortex. J Neurosci. 1995; 15:8234–8245. [PubMed: 8613757]

Scanziani M, Gähwiler BH, Charpak S. Target cell-specific modulation of transmitter release at terminals from a single axon. Proc Natl Acad Sci USA. 1998; 95:12004–9. [PubMed: 9751780]

Shahlaie K, Lyeth B, Gurkoff GG, Muizelaar JP, Berman RF. Neuroprotective Effects of Selective N-Type VGCC Blockade on Stretch Injury-Induced Calcium Dynamics in Cortical Neurons. J Neurotrauma. 2010; 27:175–87. [PubMed: 19772476]

Somogyi P, Tamás G, Lujan R, Buhl EH. Salient features of synaptic organisation in the cerebral cortex. Brain Res Brain Res Rev. 1998; 26:113–35. [PubMed: 9651498]

Takahashi T, Forsythe ID, Tsujimoto T, Barnes-Davies M, Onodera K. Presynaptic calcium current modulation by a metabotropic glutamate receptor. Science. 1996; 274:594–597. [PubMed: 8849448]

Takahashi E, Ino M, Miyamoto N, Nagasu T. Expression analysis of P/Q-type Ca2+ channel alpha 1A subunit mRNA in olfactory mitral cell in N-type Ca2+ channel alpha 1B subunit gene-deficient mice. Brain Res Mol Brain Res. 2004; 124:79–87. [PubMed: 15093688]

Tseng GF, Prince DA. Epileptogenesis in chronically injured cortex: in vitro studies. J Neurophysiol. 1993; 69:1276–91. [PubMed: 8492163]

Tseng GF, Prince DA. Structural and functional alterations in rat corticospinal neurons after axotomy. J Neurophysiol. 1996; 75:248–267. [PubMed: 8822555]

Tsien RW, Lipscombe D, Madison DV, Bley KR, Fox AP. Multiple types of neuronal calcium channels and their selective modulation. Trends Neurosci. 1988; 11(10):431–8. [PubMed: 2469160]

Tsien RW, Lipscombe D, Madison D, Bley K, Fox A. Reflections on Ca(2+)-channel diversity, 1988–1994. Trends Neurosci. 1995; 18:52–4. [PubMed: 7537405]

Tsien RW, Lipscombe D, Madison DV, Bley KR, Fox AP. Multiple types of neuronal calcium channels and their selective modulation. Trends Neurosci. 1988; 11:431–8. [PubMed: 2469160]

Uematsu M, Hirai Y, Karube F, Ebihara S, Kato M, Abe K, Obata K, Yoshida S, Hirabayashi M, Yanagawa Y, Kawaguchi Y. Quantitative chemical composition of cortical GABAergic neurons revealed in transgenic venus-expressing rats. Cereb Cortex. 2008; 18:315–330. [PubMed: 17517679]

Wheeler DB, Randall A, Tsien RW. Roles of N-type and Q-type Ca2+ channels in supporting hippocampal synaptic transmission. Science. 1994; 264:107–11. [PubMed: 7832825]

Wheeler DB, Randall A, Tsien RW. Changes in action potential duration alter reliance of excitatory synaptic transmission on multiple types of Ca2+ channels in rat hippocampus. J Neurosci. 1996; 16:2226–37. [PubMed: 8601803]

Wilson RI, Kunos G, Nicoll RA. Presynaptic specificity of endocannabinoid signaling in the hippocampus. Neuron. 2001; 31:453–62. [PubMed: 11516401]

Williams ME, Brust PF, Feldman DH, Patthi S, Simerson S, Maroufi A, McCue AF, Veliçelebi G, Ellis SB, Harpold MM. Structure and functional expression of an omega-conotoxin-sensitive human N-type calcium channel. Science. 1992; 257(5068):389–95. [PubMed: 1321501]

Wu LG, Westenbroek RE, Borst JG, Catterall WA, Sakmann B. Calcium channel types with distinct presynaptic localization couple differentially to transmitter release in single calyx-type synapses. J Neurosci. 1999; 19:726–36. [PubMed: 9880593]

Wyeth MS, Zhang N, Mody I, Houser CR. Selective reduction of cholecystokinin-positive basket cell innervation in a model of temporal lobe epilepsy. J Neurosci. 2010; 30:8993–9006. [PubMed: 20592220]

Xu JH, Long L, Wang J, Tang YC, Hu HT, Soong TW, Tang FR. Nuclear localization of Ca(v)2.2 and its distribution in the mouse central nervous system, and changes in the hippocampus during and after pilocarpine-induced status epilepticus. Neuropathol Appl Neurobiol. 2010; 36:71–85. [PubMed: 19811616]

Zaitsev AV, Povysheva NV, Lewis DA, Krimer LS. P/Q-type, but not N-type, calcium channels mediate GABA release from fast-spiking interneurons to pyramidal cells in rat prefrontal cortex. J Neurophysiol. 2007; 97:3567–73. [PubMed: 17329622]

Zhang JF, Ellinor PT, Aldrich RW, Tsien RW. Multiple structural elements in voltage-dependent Ca2+ channels support their inhibition by G proteins. Neuron. 1996; 17:991–1003. [PubMed: 8938130]

Zhang SJ, Jackson MB. GABA-activated chloride channels in secretory nerve endings. Science. 1993; 259:531–4. [PubMed: 8380942]

Highlights

- Presynaptic P/Q and N-type channels mediate GABA release onto control layer V Pyr cells
- Loss of N-type calcium channels in injured inhibitory presynaptic terminals
- Lack of compensatory mechanisms in P/Q-channels in UCs

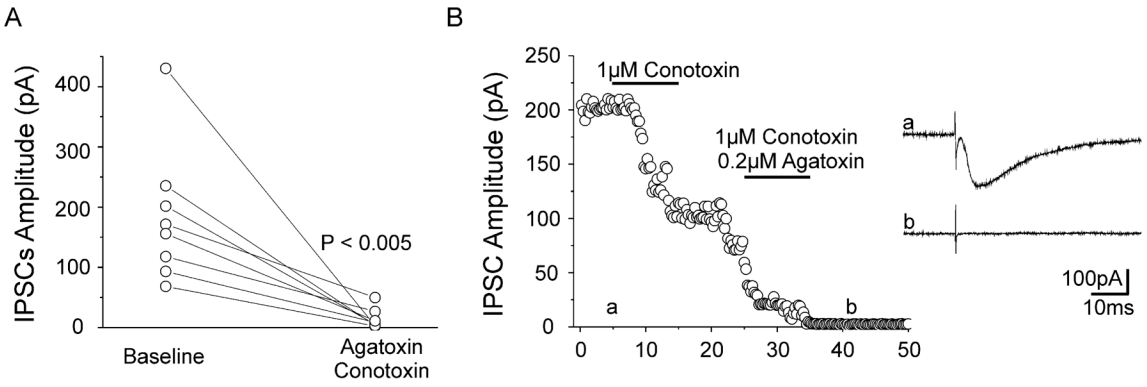

Figure 1. P/Q- and N-type channels mediate calcium influx into control presynaptic inhibitory terminals in cortical layer V

A. Plot of control eIPSC peak amplitude at baseline and 10 min after co-application of 1 μM Conotoxin and 0.2 μM Agatoxin. Each symbol: mean peak amplitude of eIPSCs recorded in standard ACSF (left) and after toxin co-treatment (right) in 8 control layer V Pyr cells. Each line connects pre- and post-toxin value for 1 cell. P<0.005 paired t-test.

B. Time series showing representative recording of monosynaptic eIPSCs from a layer V control Pyr cell sequentially exposed to conotoxin and conotoxin + agatoxin (horizontal bars: drug application). Inset: Sample eIPSCs obtained at baseline (a) and after co-treatment (b). Each symbol: single response at time point shown. Combined N- and P/Q-channel blockade successfully suppressed eIPSCs.

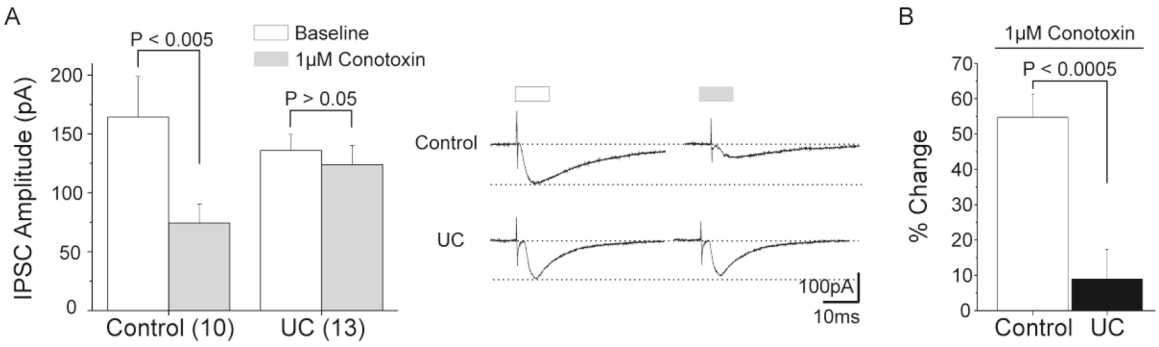

Figure 2. Effects of N-type channel blockade in layer V inhibitory terminals of control and UC cortex

A. Baseline mean peak amplitude of control eIPSCs decreased by approximately 50% after local perfusion of 1 μM ω-conotoxin GVIA (left). In contrast, no difference was observed in baseline peak amplitude of eIPSCs after treatment in UCs (right). Inset: Representative traces of eIPSCs recorded in control (upper traces) and UC (lower traces) layer V Pyr cells at baseline (white bar) and after 1 μM ω-conotoxin GVIA (gray bar).

B. Normalized changes in baseline peak amplitude of eIPSCs after N-channel blockade in layer V Pyr cells from control and UC. Change in peak amplitude of eIPSC after N-channel blockade is significantly greater in control than in UCs.

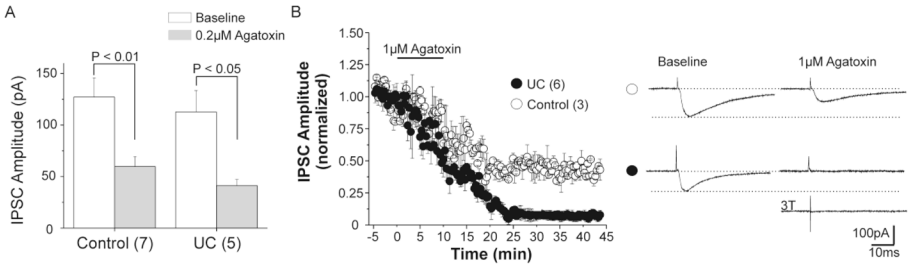

Figure 3. Effects of P/Q-channel blockade on IPSCs evoked in control and UC layer V Pyr cells

A Baseline peak amplitude of eIPSCs decreased significantly in control (left) and UC (right) layer V Pyr cells after 0.2 μM agatoxin.

B. Time series showing mean eIPSC amplitude from 3 control (open circles) and 6 UC (filled circles) Pyr cells during long term recordings after P/Q-channel blockade with increased (1 μM) agatoxin concentration. P/Q-channel blockade decreased control peak amplitude of eIPSCs by approximately 50%, similar to result with 0.2 μM agatoxin in A. Peak amplitude of eIPSCs in UC cells was markedly reduced after prolonged exposure to 1 μM agatoxin. Inset: Representative eIPSCs from control (upper traces) and UC Pyr cells (lower traces) at baseline (left) and after 1 μM agatoxin perfusion (right) showing differences in sensitivity to P/Q-channel blockade. Bottom right: sample trace from UC neuron showing persistent failure of eIPSC to increased stimulus width (3T).

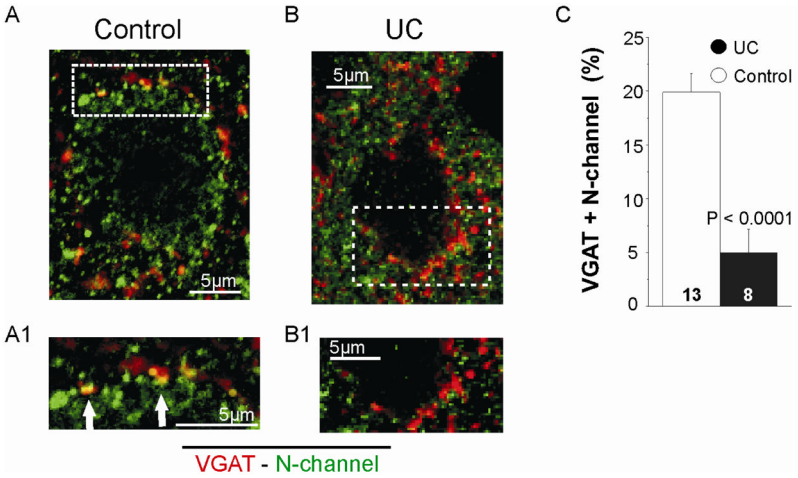

Figure 4. Decreased perisomatic density of N-type channels in UC inhibitory terminals

A. Image of confocal section through center of a control layer V Pyr cell. Dual immunoreactivity for VGAT (red) and N-channel (green) is colocalized (yellow) in control inhibitory presynaptic terminals. A1. Image of boxed area in A at higher magnification and increased contrast shows co-localized pixels in control perisomatic region more clearly (arrows).

B. Confocal image showing lack of perisomatic colocalization of VGAT- and N-channel-IR in perisomatic terminals of an UC Pyr cell. B1. Confocal image of boxed area in B at higher magnification and increased contrast.

C. Mean percentage of perisomatic colocalization of VGAT and N-channel-IR for 13 control and 8 UC Pyr cells in layer V. Here and in Figs. 5, 6, results are expressed as total immunoreactivity area/area of perisomatic region of interest and normalized (see Methods)

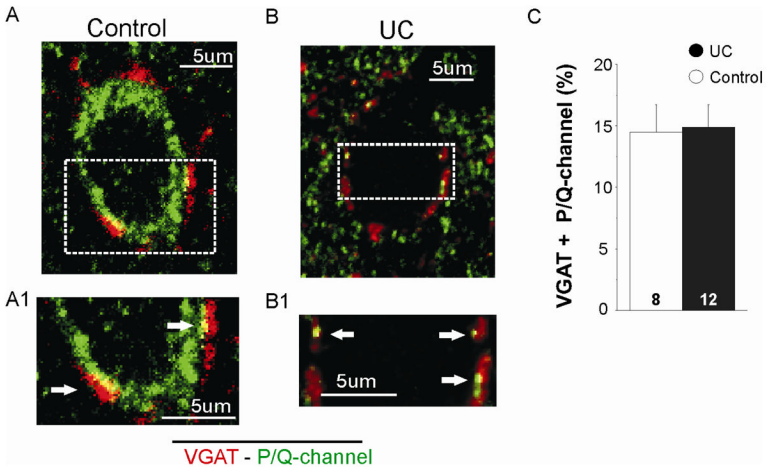

Figure 5. Perisomatic density of P/Q-type channels in inhibitory terminals from control and UCs

A. Perisomatic colocalization (yellow) of VGAT- (red) and P/Q-channel-IR (green) present in control inhibitory presynaptic terminals. A1. Boxed area of A shown at higher magnification to better visualize co-localized pixels in control perisomatic region (arrows).

B. Representative image from UC cell showing perisomatic colocalization of VGAT- and P/Q-channel-IR (yellow) similar to that of A. B1. Boxed area of B at higher magnification to visualize co-localized pixels in control perisomatic region (arrows).

C. Means for perisomatic co-localized IR for VGAT + P/Q-channels are similar in control and UCs (unpaired t-test; $P > 0.05$).